THE FINE STRUCTURE OF PROLIFERATING CELLS IN PRENEOPLASTIC RAT LIVERS DURING AZO-DYE CARCINOGENESIS

SHUICHI KARASAKI

From the Laboratoires de Recherche, Institut du Cancer de Montréal, Hôpital Notre-Dame, and Département d'Anatomie, Université de Montréal, Montréal, Canada

ABSTRACT

The continuous feeding of the carcinogenic aminoazo dye DAB to rats produces hyperbasophilic foci in the preneoplastic livers. After injections of thymidine-^{3}H into the rats, such foci were isolated from the livers and studied by radioautography with the phase-contrast and electron microscopes. In these foci, the only cells found to be proliferating, as determined by the uptake of thymidine-^{3}H into their nuclei, were a poorly differentiated type; well differentiated hepatocytes in the same regions were not labeled with the isotope. The labeled cells had an irregular cell outline and a high nucleocytoplasmic ratio; the cytoplasm had almost completely lost the specialized elements characteristic of hepatocytes; the irregular nuclei with prominent nucleoli, the altered mitochondria, and the increased free ribosomes noted in these cells are features which are characteristic of neoplastic cells induced by DAB. Thus, it seems likely that the hyperbasophilic foci represent the sites of extensive dedifferentiation of hepatocytes followed by rapid cellular proliferation, leading to neoplastic growth.

INTRODUCTION

Studies on preneoplastic rat livers have revealed that the administration of the carcinogenic aminoazo dyes initially induces extensive destruction of parenchymal tissue. This change is soon followed by a regenerative process leading to the formation of cirrhotic livers, i.e. the development of nodules of hyperplastic parenchyma surrounded by trabeculae of bile ducts and connective tissue (4, 8, 9, 11, 12, 16, 22, 24, 29–31). Some areas of the hyperplastic nodules are then observed to stain intensely with basic dyes, and significant increases in the rates of DNA synthesis and cell proliferation occur in these sites, suggesting that such hyperbasophilic foci may represent the sites of origin of hepatomas (8, 9, 22, 25, 30, 36).

The fine structure of the hepatocytes in aminoazo dye–fed animals has been investigated by several authors, but those ultrastructural studies have dealt either with cellular alterations occurring at very early stages of aminoazo dye feeding (4, 12, 16, 20, 33) or with alterations occurring in the developing tumors (21, 29, 39). No electron microscopic investigation has been carried out thus far, to the best of the author's knowledge, on the hepatocytes of the hyperbasophilic foci.

In the present work, the ultrastructure of the hyperbasophilic cells has been examined for determining whether they actually represent the transition between hyperplasia and neoplasia. As seen by electron microscopy, the neoplastic hepatocytes differ radically from the hepatocytes of normal and cirrhotic livers (6, 14, 15, 21, 26–29, 35, 39),

and one could expect many characteristics of the neoplastic cells to appear in cells of the hyperbasophilic foci if the latter are the sites of the neoplastic transformation. Moreover, the proliferating cells of these regions were distinguished from the resting cells by thymidine-^{3}H radioautography in order to study the ultrastructure of these two cell types differentially.

MATERIAL AND METHODS

Animals

Male, adult, albino rats (Wistar strain) were fed for 3–5 months a semisynthetic diet (diet 3 of Miller et al. [24]) which contained the carcinogenic aminoazo dye, *N*, *N'*-dimethyl-4-aminoazobenzene (DAB), at a concentration of 0.06%. In the experiments with radioautography, the rats received three subcutaneous injections of an aqueous solution of thymidine-^{3}H (New England Nuclear Corporation, Boston, specific activity: 6.7 c/mmole). The injections were given at 1.5-hr intervals at a dose of 0.5 μc per g body weight. The animals (200–250 g) received a total dose of 1.5 μc per g body weight.

Preparation of Tissues

The rats were sacrificed by ether inhalation at 6 hr after the first injection. The livers were excised and cut into slices about 0.5 mm thick with a razor blade. The thin slices were immediately transferred to a Petri dish containing 3.0% glutaraldehyde in 0.07 M cacodylate buffer at pH 7.2. During fixation, samples were picked up from the slices with a glass capillary 0.5–1 mm in diameter. The samples were taken from small, whitish areas suspected of being hyperbasophilic foci, as well as from surrounding liver tissue and hepatomas. The sites of the different punctures were precisely recorded on a diagram, and the samples were transferred into vials containing fresh fixative. After 2-hr fixation, the samples were washed for another 2 hr in the buffer solution and postfixed for 2 hr in 1% OsO_4 in acetate Veronal buffer at pH 7.2. Finally, they were dehydrated in graded alcohols and embedded in Epon.

The punctured slices were fixed for 4 hr in glutaraldehyde and kept overnight in cacodylate buffer. They were then dehydrated, cleared, and embedded in paraffin. Semiserial sections, 5 μ thick, were cut from the punctured slices and stained with 0.1% toluidine blue in Veronal buffer at pH 5.0 (9) or with Harris' hematoxylin. Sections stained with hematoxylin were covered with Kodak NTB-2 emulsion by the dipping technique (36). After 2 wk of exposure, the radioautographs were developed in Dektol and fixed with Rapid Fixer (Eastman Kodak Co., Rochester, N. Y.).

Examination of the Isolated Samples

Thick (0.5–1-μ) sections were prepared from Epon-embedded material with a Porter-Blum microtome. The sections deposited on a glass slide were covered with Kodak NTB-2 emulsion by the dipping technique (36) and exposed for 2 wk. They were then developed in Dektol, fixed in Rapid Fixer, and examined under a phase-contrast microscope with the Heine condenser.

Thin (0.02–0.05-μ) sections were cut and mounted on formvar-coated grids and examined with an RCA-EMU-3C electron microscope. In the experiments with electron microscope radioautography, the sections were coated with a thin film (~0.1 μ) of Ilford L-4 emulsion by an expandable loop method (18). After exposure for 3–5 months, the radioautographs were developed in Microdol-X at 20° for 4 min, fixed in Rapid Fixer, and stained with Karnovsky's alkaline lead for 15 min (18).

OBSERVATIONS

Identification of the Samples Derived from Basophilic Parenchyma, Hyperbasophilic Foci, and Hepatomas

The type of parenchymal cells included in the samples used for ultrastructure studies was identified by light microscopic examination of sections of the punctured slices stained by toluidine blue. Fig. 1 shows, for example, that a puncture was made in a region which stains intensely with toluidine blue. This region showed a relatively high nucleocytoplasmic ratio, and the radioautograph prepared from the adjacent section revealed a high rate of thymidine-^{3}H incorporation, but the region did not invade or displace the surrounding tissue. This area thus differs radically from the surrounding parenchymal tissue, but could not be considered a tumor. It was classified as a hyperbasophilic focus and electron microscope studies were made on this and similar samples which apparently consisted of hyperbasophilic cells. The results obtained with such samples were compared with those obtained with samples from basophilic parenchymal nodules and from hepatomas (trabecular and adenomatous) identified in a similar manner.

Different Cell Types in Hyperbasophilic Parenchyma

Examination under phase-contrast microscopy of thick (0.5–1 μ) sections from samples of hyper-

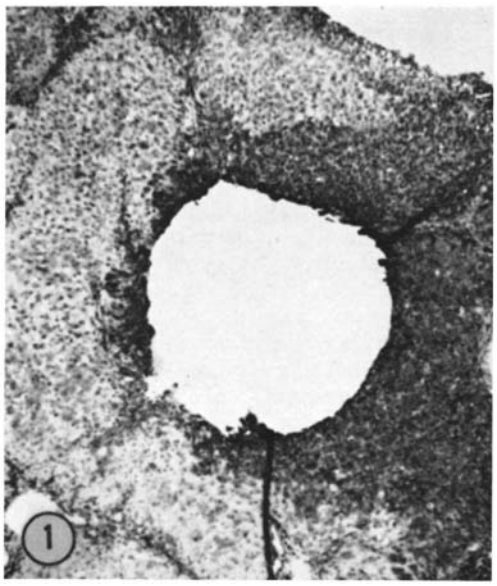

FIGURE 1 Light micrograph of a liver slice indicating the site of isolation of a sample for fine-structural examination. The slice was obtained from the liver of a DAB-fed rat which was injected with thymidine-^{3}H. During the fixation with glutaraldehyde, the parenchyma was taken from the punctured area. In the histological section stained with toluidine blue (pH 5.0), it is confirmed that the puncture was made in a hyperbasophilic focus. × 35.

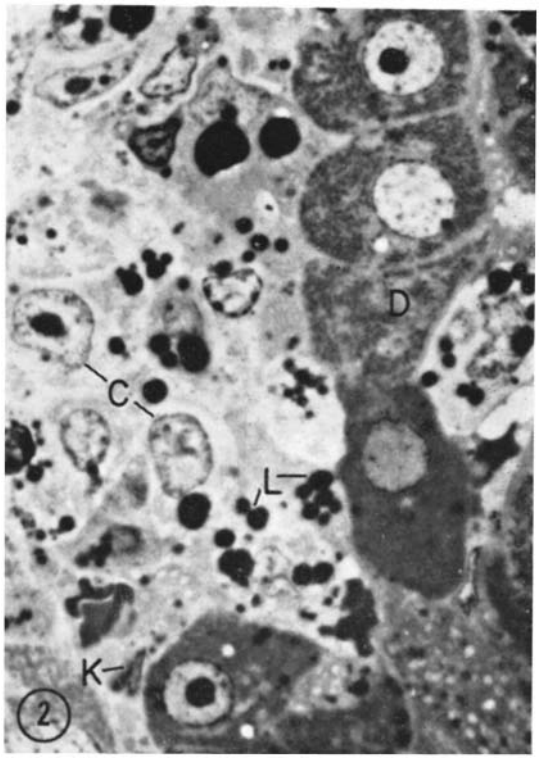

FIGURE 2 Phase-contrast micrograph of a thick section of the isolated hyperbasophilic region. "Dark" cells (*D*) are characterized by the round nucleus and opaque mitochondria and are arrayed in a trabecular pattern. "Clear" cells (*C*) containing the irregular nucleus and pale cytoplasm are present without any particular arrangement. Lipoid droplets (*L*); Kupffer cell (*K*). 1-μ section was cut from a block prepared for electron microscopy and was stained with toluidine blue (pH 10). × 1,100.

basophilic parenchyma revealed that two different cell types could be distinguished in hyperbasophilic foci. According to the opacity of their cytoplasm, hepatocytes of these regions were classified as "dark" or "clear" cells (Fig. 2).

Under phase contrast, the dark cells did not differ significantly from normal hepatocytes or from hepatocytes of the basophilic parenchyma surrounding the hyperbasophilic foci in DAB-fed rats. They usually showed a regular polygonal outline and were arranged in trabecular or epithelial pattern. Their nuclei were usually round in shape, contained at least one round nucleolus, and were surrounded by a large cytoplasmic mass. Apparently, the dark character of these cells was due mainly to the abundance of opaque mitochondria. The clear cells, on the other hand, differed remarkably from hepatocytes of the normal liver and from hepatocytes of the surrounding basophilic tissue in DAB-fed animals. They varied greatly in size and shape and showed no particular type of arrangement. Their nuclei were rather elongated and irregular in shape. The nucleocytoplasmic ratio was relatively high in these cells, and nucleolar hypertrophy was conspicuous. The cytoplasm contained an appreciable number of lipoid droplets. The mitochondria did not show up under phase contrast in this cell type. Cells with a similar appearance were also detectable in the developing hepatomas.

The small hyperbasophilic foci (less than 0.5 mm in diameter) consisted mainly of dark hepatocytes. Clear cells were scattered as single cells or groups of two to three cells (Fig. 3) and represented about 10% of the total number of cells in the preparation. In larger hyperbasophilic foci (less than 2.0 mm in diameter), the clear cells occupied

relatively larger areas (Fig. 4) and accounted for up to 75% of the total number of hyperbasophilic cells. In small hepatomas (less than 6 mm in diameter) the "clear" cells always occurred more frequently than the "dark" cells.

Both the dark and the clear cells could be easily distinguished from other cell types such as Kupffer cells, cells of the bile ducts, and cells of connective tissue included in samples of hyperbasophilic foci. The nuclei of dark and clear cells had mean diameters of 7.0 and 7.8 μ, respectively, as estimated by ocular micrometry. A similar value, 7.5 μ, was reported for nuclei of normal hepatocytes (7). In contrast, the mean diameters of nuclei in other cell types ranged from 3 to 5 μ.

Incorporation of Thymidine-^{3}H into the Nuclei of the Different Cell Populations

Examination of radioautographs under phase contrast revealed that 1.3% of the nuclei in nodules of basophilic parenchyma were labeled at 6 hr after injections of thymidine-^{3}H (Table I). In hyperbasophilic foci, very few dark cells were found to be labeled and the thymidine-^{3}H uptake was limited almost exclusively to the clear cells (Figs. 3 and 4). The latter showed incidences of nuclear labeling varying from 16.1 to 63.5% in samples from different hyperbasophilic regions. In hepatomas, both dark and clear cells showed high percentages of labeled nuclei.

The Fine Structure of the Different Cell Types in Hyperbasophilic Foci

Examination of specimens by electron microscopy confirmed the observation made by phase-contrast microscopy that two different cell types, dark and clear cells, could be easily distinguished in hyperbasophilic parenchyma on the basis of the shage and opacity of their mitochondria. The fine structure of each cell type will be described separately.

DARK CELLS: The dark cells of hyperbasophilic foci exhibited ultrastructural characteristics similar to those of the basophilic hepatocytes in neighboring tissue. The nuclei were round or oval

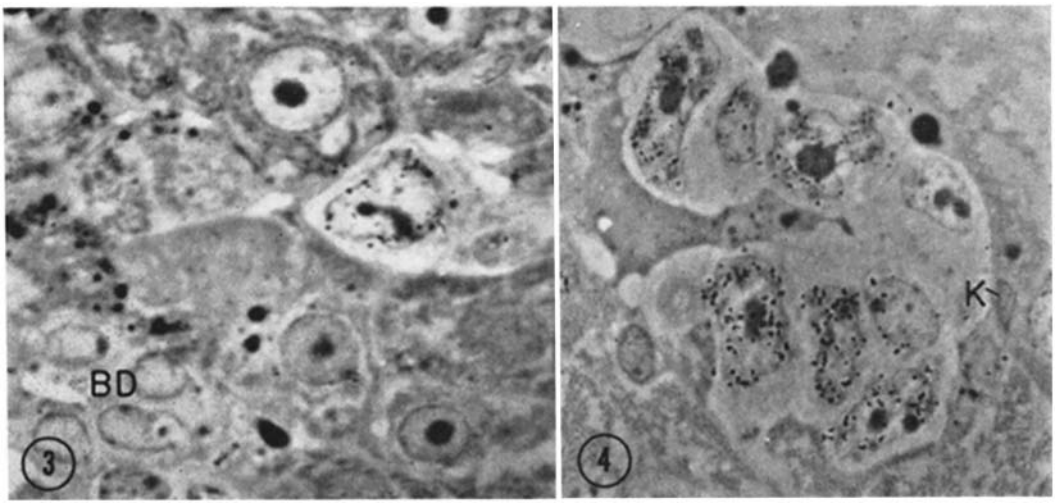

FIGURES 3 and 4 Radioautographs of thymidine-^{3}H-labeled cells in the hyperbasophilic foci, seen under the phase-contrast microscope. Silver grains of NTB-2 emulsion were developed in Dektol. Unstained sections.

FIGURE 3 A single clear cell is surrounded by dark hepatocytes. The grains are located over the large nucleus of the clear cell. A biliary duct (*BD*). × 1,100.

FIGURE 4 Labeled clear cells are arranged in a group. A Kupffer cell (*K*). × 1,100.

TABLE I

Percentages of Labeled Nuclei in Different Cell Types of the Preneoplastic and Neoplastic Liver Parenchyma 6 Hr after Thymidine-^{3}H Injection

Cellular population		"Dark" Cell			"Clear" Cell		
		No. of counted nuclei	No. of labeled nuclei	%	No. of counted nuclei	No. of labeled nuclei	%
Basophilic		1678	21	1.3	—	—	—
Hyperbasophilic	(a)	291	3	1.0	31	5	16.1
	(b)	451	4	0.9	161	74	46.0
	(c)	440	0	0	511	192	37.6
	(d)	275	0	0	507	322	63.5
	(e)	224	0	0	659	264	40.1
Hepatoma		1166	125	10.7	1097	103	18.5

(a)–(e) Samples from different hyperbasophilic foci.

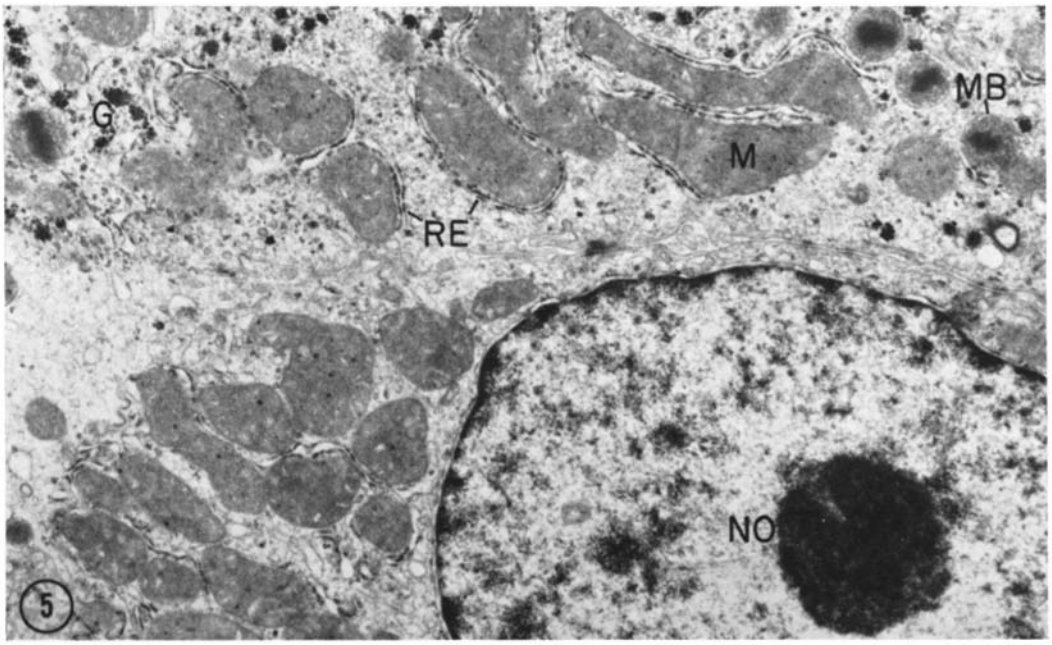

FIGURES 5–13 Electron micrographs of cells in the hyperbasophilic foci. The thin sections were coated with Ilford-L-4 emulsion for radioautography. Stained with alkaline lead.

FIGURE 5 Dark hepatocyte. The nuclei of this cell type were found to be unlabeled with thymidine-^{3}H. The cytoplasm exhibits opaque mitochondria (*M*), rough endoplasmic reticulum (*RE*), microbodies (*MB*), and glycogen granules (*G*). The nucleus contains a round nucleolus (*NO*). The chromatin material is accumulated along the nuclear envelope. × 18,000.

in shape without noticeable indentation (Fig. 5). The nucleolus was round and made up of anastomotic strands of fibrillar and particulate components. The chromatin was relatively uniform in distribution, although higher concentrations were observed near the nuclear membrane and around the nucleolus. Interchromatin and perichromatin granules were detectable in the nucleoplasm.

The mitochondria were abundant and had a homogeneous matrix of moderate opacity (Figs. 6 and 7). The internal cristae varied in length, but were generally short relative to the width of the organelles. Intramitochondrial granules, 200–500 A in size, were usually found in the matrix.

The smooth endoplasmic reticulum was frequently arranged in prominent clusters, and glycogen was occasionally scattered among the membranes of smooth endoplasmic reticulum (Fig. 6). Profiles of rough endoplasmic reticulum occurred singly, with little tendency to form parallel arrays, and were often localized in close proximity to mitochondria (Fig. 7). Ribosomes were found in clusters of four to ten lying in the cytoplasmic matrix. The Golgi complex, microbodies, lysosomes, and lipoid bodies were present in varying frequency. Biliary canaliculi and the associated desmosomes were also present.

CLEAR CELLS: The clear cells were recog-

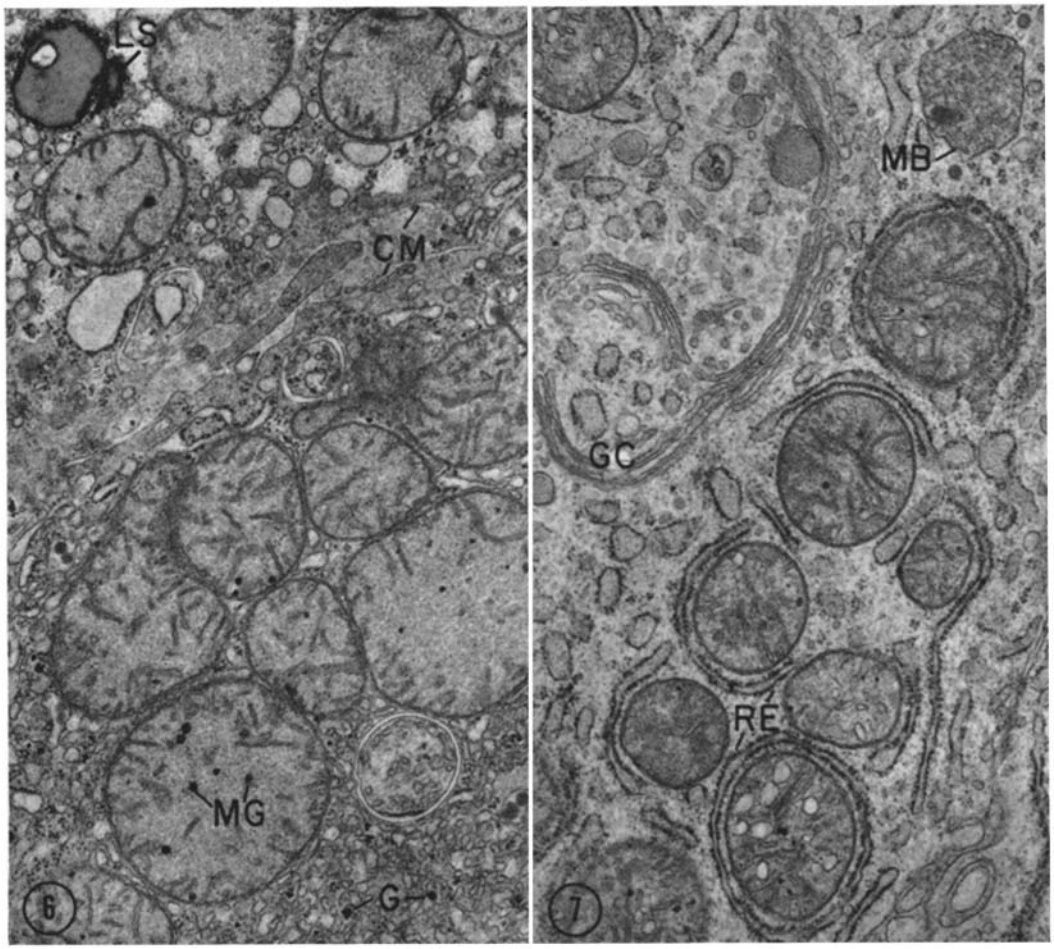

FIGURE 6 Boundary region between two adjoining dark hepatocytes. The mitochondria exhibit normal platelike cristae of varying length that are short with respect to the width of the organelles; a few triangular and circular profiles of cristae are also seen. The intercristal matrices consist of homogeneous substance with moderate density and also contain many intramitochondrial granules (*MG*). A few glycogen granules (*G*) are scattered among the membranes of smooth endoplasmic reticulum. A lysosome (*LS*) and many vesicles are located in the vicinity of the cell membrane (*CM*). × 30,000.

FIGURE 7 Perinuclear cytoplasm of a dark hepatocyte. The mitochondria exhibit many cristae. The opaque intercristal matrix contains a few mitochondrial granules. Cisternal profiles of rough endoplasmic reticulum (*RE*) wrap around mitochondria. Golgi complex (*GC*); microbody (*MB*). × 30,000.

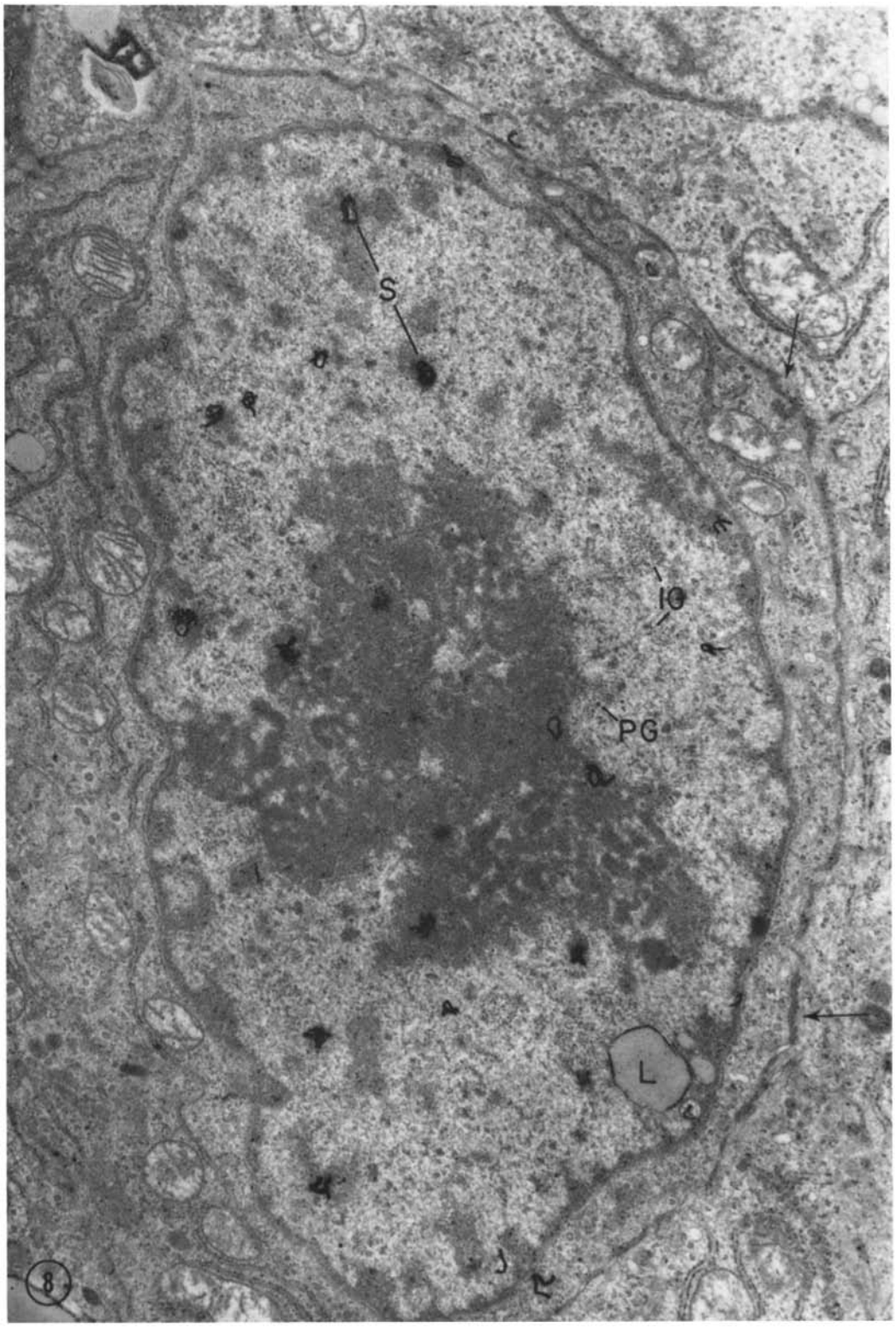

FIGURE 8 A labeled clear cell of the hyperbasophilic region. Many silver grains (*S*) over the nucleus are preferentially associated with the chromatin clumps. Six silver grains are also found over the large nucleolus. Many clusters of interchromatin granules (*IG*) are present. Perichromatin granules (*PG*) are also frequently detectable. Intranuclear lipoid bodies (*L*) are situated in close association with the condensed chromatin. Mitochondria are pale; their cristae are clearly defined. Rough endoplasmic reticulum is scanty in amount and tends to be at the side of mitochondria. Free ribosomes are numerous in the cytoplasmic matrix. The cellular boundaries (arrows) appear as an interrupted dark band. × 20,000.

nized under the electron microscope by the presence of lightly stained mitochondria and by nuclear labeling with thymidine-^{3}H (Fig. 8).

The interphase nuclei of clear cells were irregular in shape and the nuclear envelope showed a ruffled pattern. Clumps of chromatin were often found along the nuclear membrane, in the center of the nucleus, or in close contact with the nucleolus. Loosely distributed fibrils found in interchromatin areas were similar to those present in condensed chromatin areas. Clusters of interchromatin granules were frequent and often were found intermingled with dispersed chromatin fibrils. Many perichromatin granules were also present in condensed chromatin. Lipoid droplets similar to those observed in the cytoplasm were commonly associated with the condensed chromatin. In labeled nuclei, the silver grains were frequently located above the condensed chromatin rather than above the interchromatin areas. The nucleolus was usually large, loosely constructed, and reticulated with prominent granular and fibrous regions (Fig. 8). The granular regions consisted of particulate components 100–150 A in diameter, while the fibrous regions appeared as dense aggregates of fibrous material intermingled with some particulate components. The presence of silver grains above the nucleoli suggested the existence of intranucleolar chromatin.

The mitochondria showed important variations in size and shape. Their matrices were generally pale and intramitochondrial granules were absent (Fig. 9). The cristae were irregularly developed and showed both lamellar and circular profiles (Fig. 10).

The rough endoplasmic reticulum was scattered throughout the cytoplasm. No organized arrays of parallel profiles were found and the single cisternae were usually curved around the mitochondria (Fig. 9). Smooth endoplasmic reticulum was rare

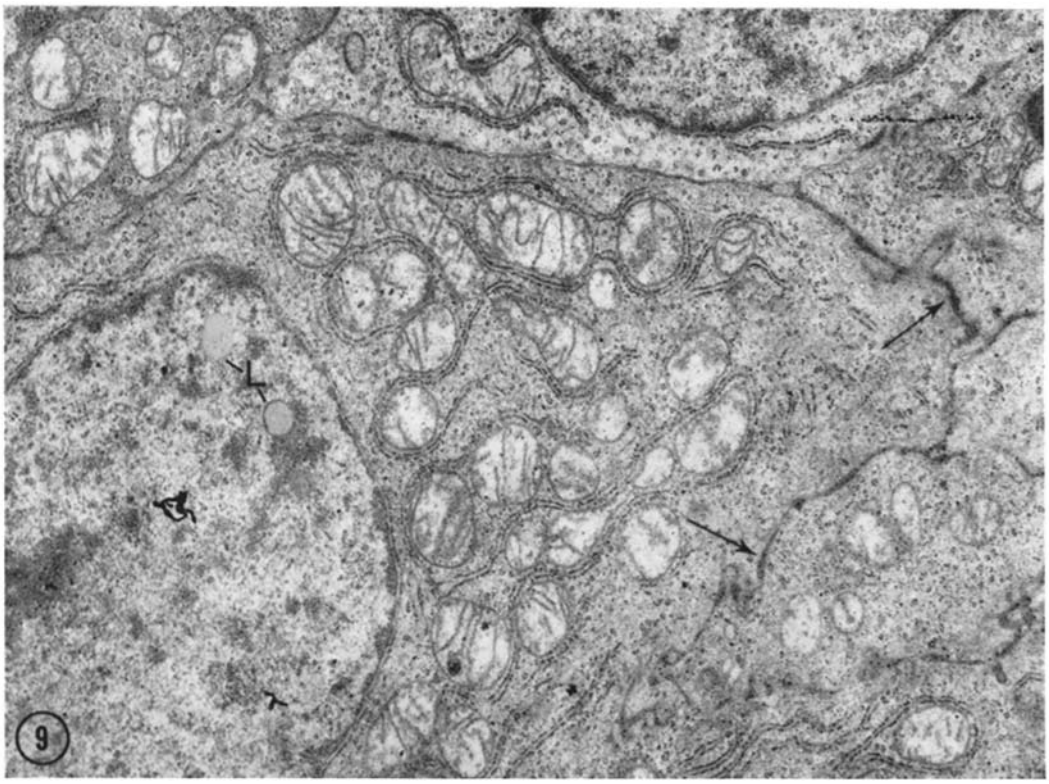

FIGURE 9 Labeled cells. The cytoplasm exhibits the close association between mitochondrial and rough endoplasmic reticulum. The mitochondrial body displays the pale matrix and lamellar cristae. Numerous free ribosomes are scattered. A dense substance is accumulated along the cellular boundaries (arrows). Intranuclear lipoid bodies (*L*). × 18,000.

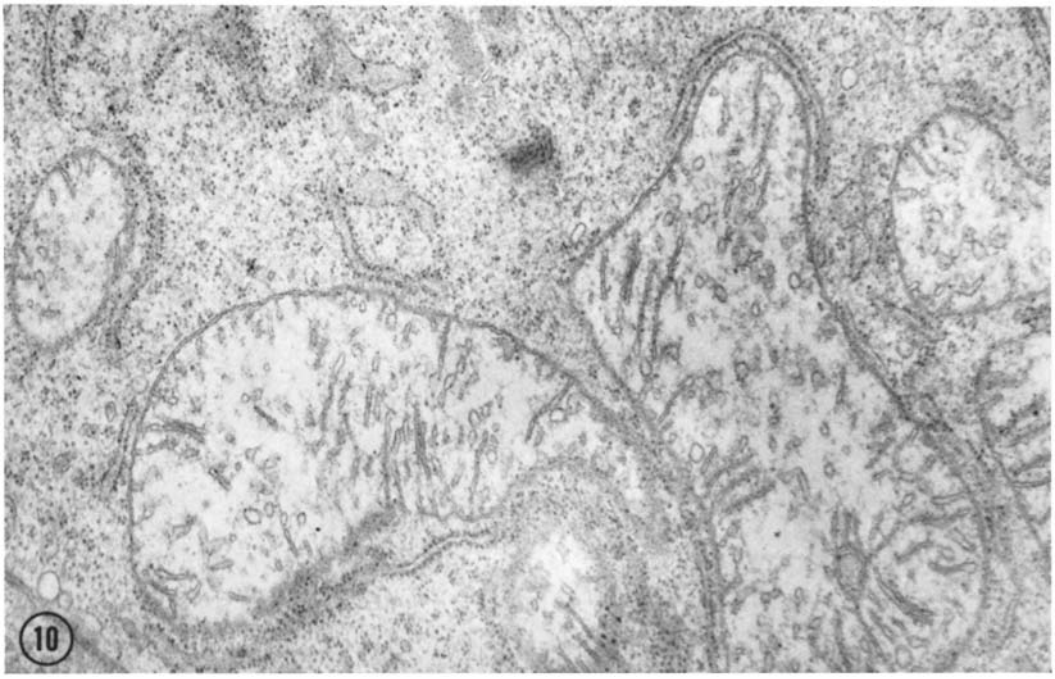

FIGURE 10 Small part of a labeled cell. Giant mitochondria exhibit the laminar and circular profiles of cristae. Intercristal matrices appear pale and quite inconspicuous. Intramitochondrial granules are entirely lacking. Numerous free ribosomes are scattered throughout the cytoplasm. A few profiles of rough endoplasmic reticulum are located in close proximity to mitochondria. × 30,000.

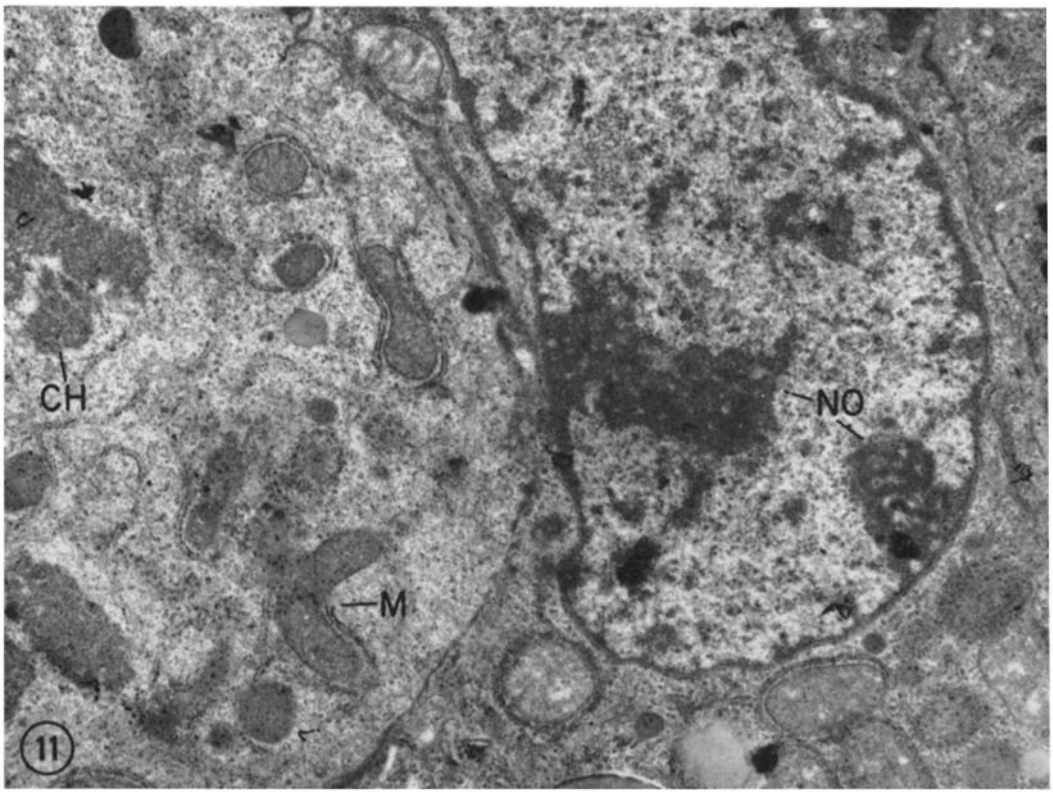

FIGURE 11 Labeled cells in metaphase and interphase. The metaphase figure of a dividing cell (left) is recognizable by the arrangement of condensed chromosomes (*CH*) and the disappearance of the nuclear envelope. Silver grains are seen over the chromosomes. In contrast to interphase (right) mitochondria, the metaphase mitochondria (*M*) show matrices of high opacity. Nucleoli (*NO*) in the interphase nucleus. × 14,000.

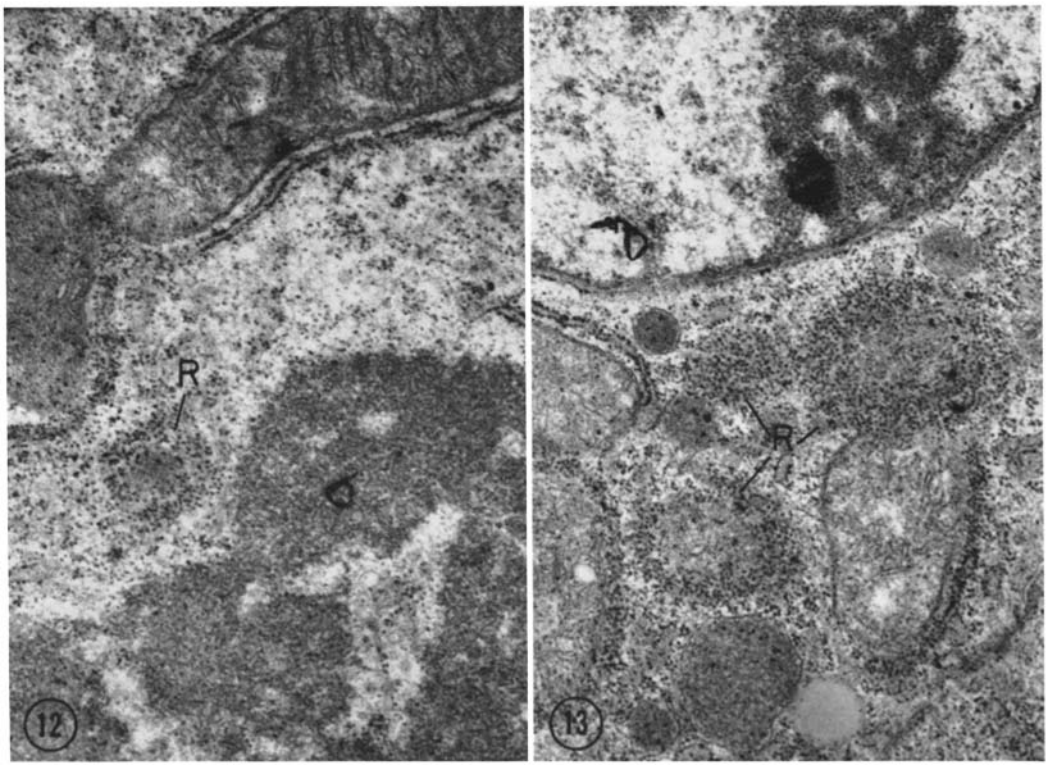

FIGURE 12 Part of the metaphase cell. An aggregate of numerous ribosomal particles (*R*) is localized near the chromosomes. Note the elongated mitochondrion with an opaque matrix. × 30,000.

FIGURE 13 Part of the interphase cell in Fig. 11. Ribosome bodies (*R*) are seen in perinuclear cytoplasm. The mitochondria exhibit a less opaque matrix. × 30,000.

and was represented by disorganized vesicles. Free ribosomes, about 150 A in size, were abundant and widely dispersed in the cytoplasmic matrix (Fig. 9). Clusters of ribosomes were frequently observed, especially in the perinuclear cytoplasm (Fig. 13).

Lipoid droplets scattered in the cytoplasm varied considerably in size and contained amorphous material of moderate opacity. Lysosomes were rarely seen. Microbodies and glycogen granules were absent. The Golgi complex was often well developed with multiple contiguous lamellae and vesicles.

The intercellular spaces among the clear cells were generally filled with a dense substance stainable by lead hydroxide (Fig. 9). Specialization of the cell membrane with the formation of microvilli of biliary canaliculi, terminal bars, and desmosomes for biliary canaliculi was not detected on the surface of labeled cells. None of the clear cells was associated with a basement membrane on the surface.

In dividing cells, chromosomes were easily recognized standing out clearly against a background of granular material (Fig. 11). Small lipoid droplets were often located within chromosomal masses. When nucleoli disappeared at metaphase, several clusters of particles 150 A in size were found at the periphery of the chromosome masses (Fig. 12). These granular aggregates persisted within the perinuclear cytoplasm for a time after reconstitution of the nuclear envelope (Fig. 13). They might correspond to the "ribosome bodies" which Jones (17) found in mitotic division of erythroblasts. In contrast to the interphase mitochondria (Fig. 13), the mitochondria found at metaphase were of higher opacity (Fig. 12). The other cyto-

plasmic organelles showed no particular variation in fine structure during cell division.

DISCUSSION

Morphological examination of the preneoplastic liver parenchyma during DAB carcinogenesis has indicated that two different cell types, dark and clear cells, are present in hyperbasophilic foci. The dark cells retain the major ultrastructural characteristics of typical hepatocytes reported previously (5, 26, 27, 34, 35); they are also cytologically similar to the hepatocytes in the basophilic parenchyma surrounding hyperbasophilic foci in DAB-fed animals (4, 20, 29, 33, 39). The clear cells, on the other hand, bear a close ultrastructural resemblance to the poorly differentiated neoplastic cells found in primary hepatomas induced by the carcinogenic aminoazo dyes (19, 21, 26, 29, 39). In addition, like the hepatoma cells (22, 36, 37), these clear cells incorporate appreciable amounts of thymidine-^{3}H, indicating that they constitute a rapidly proliferating cell population.

Recently, the fine structure of hyperplastic liver nodules which might be preneoplastic was studied in 2-fluorenylacetamide-fed rats by Merkow et al. (23) and in aging C3H mice by Essner (10). Although the hepatocytes of the nodules were found to differ ultrastructurally from the extranodular hepatocytes, these cells retained the major characteristics of typical hepatocytes. On the other hand, atypical cells similar to the clear cells reported in this paper were not described by either of these authors. It should be emphasized, however, that even in the present studies these clear cells were not observed in all of the basophilic parenchymal nodules induced by DAB, but only appeared within the hyperbasophilic foci representing the specific areas in preneoplastic liver parenchyma.

Dauost and Molnar (9) have previously reported that cells in some hyperbasophilic foci show various cytological features of cancer cells, such as nucleolar hypertrophy, irregularity of the nuclear outline, increased mitotic figures, and high nucleocytoplasmic ratio. The present study has confirmed these findings, particularly in the clear cells labeled with thymidine-^{3}H. In addition, electron microscopy reveals that the nuclear alterations are frequently accompanied by the formation of prominent chromatin clumps and occasionally are associated with apparent increases in the numbers of interchromatin and perichromatin granules. The enlarged nucleoli are loosely constructed and reticulated with prominent particulate components. All these fine structural characteristics are comparable to the features of neoplastic nuclei, recently reviewed by Bernhard and Granboulan (3). Similar features, however, have also been recognized by Stenger and Confer (38) in the nuclei of regenerating rat livers; these authors have stressed that such alterations of neoplastic nuclei are more likely to be associated with a rapid rate of cellular proliferation than with any intrinsic properties of neoplasia. The same generalization appears to apply for the nuclei of clear cells in the hyperbasophilic foci.

The cytoplasmic structure of the clear cells shows more significant alterations. The clear cells are characterized by the uniform absence of specific organelles such as smooth endoplasmic reticulum, microbodies, biliary canaliculi, and glycogen granules, which might indicate the previous state of cellular differentiation of the hepatocytes (5, 26, 27, 35). The mitochondria also lack their opaque matrix substance and intramitochondrial granules which are usually observed in hepatic mitochondria after fixation with glutaraldehyde and osmium tetroxide (5). Parallel arrays of cisternae of the rough endoplasmic reticulum, which are typical of many secretory cell types, including hepatocytes (5, 26, 27, 32, 34, 35), are not observed in the clear cells. In contrast to the relative exclusion of other organelles, the cytoplasm of clear cells possesses a high concentration of free ribosomal particles. A similar feature of cytodifferentiation was reported in liver cells at very early stages of embryonic development (14, 26). From a morphological viewpoint, the clear cells seem to be poorly differentiated and deficient in specialized cytoplasmic organelles. Thus, in their structural characteristics, the proliferating cells in the foci are basically different from those of regenerating liver (2, 38). The latter hepatocytes are apparently capable of maintaining a high degree of cytoplasmic organization during the phase of DNA synthesis as well as during cytokinesis (2).

It is well known that conspicuous proliferation of biliary ductal cells also occurs throughout the entire course of DAB administration (37). Farber (11) and recently Inaoka (16) reported various deviations of these newly formed cells in studies of so called "oval" cells. Furthermore, electron mi-

croscopy conclusively demonstrated the bile ductal nature of these cells (12, 16). The clear cells, on the other hand, are distinguishable from normal and proliferating biliary ductal cells by their larger mitochondria and the absence of a basement membrane as well as by the connection between adjacent cells.

It has been generally accepted that malignant cells are usually less differentiated than the cells from which they originated (26, 28). In transplantable rat hepatomas, Dalton (6) and Hruban et al. (15) found that the degree of cellular differentiation was inversely related to the rapidity of neoplastic growth as well as to the degree of malignancy. In this respect, the ultrastructural features of clear cells in the hyperbasophilic foci are comparable to those of neoplastic cells in the most rapidly growing hepatomas. Therefore, the clear cells might already have acquired almost all the cytological characteristics of an advanced malignant cell, while neither outgrowth nor metastasis could be recognized histologically. This observation supports the view, previously expressed by Daoust and Molnar (9), that hyperbasophilic foci represent the sites of neoplastic transformation during DAB carcinogenesis.

At the same time that the clear cells were becoming more prominent in the foci, a greater percentage of them could be labeled with thymidine-^{3}H (Table I, also 36). This finding indicates that the increase in clear cells was the result of proliferation of cells of the same type. Whether clear cells are stem cells or are derived from preexisting parenchyma by local dedifferentiation cannot be determined by this study. However, it seems likely that most, if not all, of the clear cells arise from hepatocytes in the foci, for two reasons. First, clear cells are more like hepatocytes with respect to the nuclear and mitochondrial sizes and the connection between adjacent cells than any other cell types which might migrate into the foci. Secondly, dark hepatocytes which occupied many parts of the foci show certain signs of dedifferentiation, as recognized by the loss of the organized endoplasmic reticulum, mitochondrial matrix, glycogen, as well as cell surface specialization (19).

Such a dedifferentiation could occur as the result of accelerated multiplication of hyperbasophilic hepatocytes, if the succession of mitoses was too rapid to allow complete maturation of cellular organelles. According to Becker and Lane (1), the response of mammalian hepatocytes to a stimulus to cell division after partial hepatectomy may be based upon dedifferentiative alterations of some cytoplasmic organelles during the early phase of preparation for cell division. In the regenerating limbs of *Ambystoma* larva, Hay and Fishman (13) reported that the nuclei began to synthesize DNA during the very early phase of dedifferentiation of tissues, although the most active multiplication of cells occurred near the end of the dedifferentiation. Similarly, dark hepatocytes which might be dedifferentiating in the hyperbasophilic foci would be expected to show a high incidence of thymidine-^{3}H–labeled nuclei if they actively participate in the formation of clear cells by cell divisions. In the present radioautographic data, however, dark hepatocytes have not been found to incorporate thymidine-^{3}H into their nuclei. Only clear cells incorporate the isotope into nuclear DNA; frequent mitoses are observed among these cells. Therefore, it seems likely that a very few hepatocytes at the beginning have undergone the dedifferentiation as a consequence of accelerated cellular proliferation. Alternatively, another possible explanation is that, during the phase of dedifferentiation of hepatocytes, there might be an inhibition of cell multiplication followed later by a burst of mitoses in the dedifferentiated cells.

A final consideration concerns the participation of proliferating clear cells to the histogenesis of hepatic neoplasia. According to Svoboda (39) and Ma and Webber (21), almost all of the hepatomas induced by the carcinogenic aminoazo dyes are a mixture of trabecular carcinoma and adenocarcinoma, the cells of which bear an ultrastructural resemblance to liver parenchymal cells and biliary duct–epithelial cells, respectively. The latter authors have also suggested, from the examination of mixed tumor patterns, an origin of the hepatic tumors from a common precursor, the differentiation of which gave rise to neoplastic cells with either parenchymal or ductal characteristics. The occurrence of primitive cells in preneoplastic livers is of interest, since these cells might be a candidate for such a common precursor.

I wish to thank Dr. Roger Daoust for continuing encouragement and advice during the course of this work. The technical assistance of Mrs. Taeko Karasaki and Miss Michelle Lahaie is gratefully acknowledged. The work was supported by grants from the National Cancer Institute of Canada.

Received for publication 13 July 1968, and in revised form 5 September 1968.

REFERENCES

1. BECKER, F. F., and B. P. LANE. 1965. Regeneration of the mammalian liver. I. Auto-phagocytosis during dedifferentiation of the liver cell in preparation for cell division. *Amer. J. Pathol.* **47**:783.
2. BECKER, F. F., and B. P. LANE. 1968. Regeneration of the mammalian liver. VI. Retention of phenobarbital-induced cytoplasmic alterations in dividing hepatocytes. *Amer. J. Pathol.* **52**:211.
3. BERNHARD, W., and N. GRANBOULAN. 1963. The fine structure of the cancer cell nucleus. *Exp. Cell Res. Suppl.* **9**:19.
4. BRUNI, C. 1960. Hyaline degeneration of rat liver cells studied with the electron microscope. *Lab. Invest.* **9**:209.
5. BRUNI, C., and K. R. PORTER. 1965. The fine structure of the parenchymal cell of the normal rat liver. I. General observations. *Amer. J. Pathol.* **46**:691.
6. DALTON, A. J. 1964. An electron microscopic study of a series of chemically induced hepatomas. *In* Cellular Control Mechanisms and Cancer. P. Emmelot and O. Muhlbock, editors. Elsevier, Amsterdam.
7. DAOUST, R. 1963. Les différentes classes de noyaux dans le parenchyme hépatique du rat au cours de la carcinogénèse. *Rev. Can. Biol.* **22**:59.
8. DAOUST, R. 1963. Cellular populations and nucleic acid metabolism in rat liver parenchyma during azo dye carcinogenesis. *In* Canadian Cancer Conference, Academic Press Inc., New York. **5**:225.
9. DAOUST, R., and F. MOLNAR. 1964. Cellular populations and mitotic activity in rat liver parenchyma during azo dye carcinogenesis. *Cancer Res.* **24**:1898.
10. ESSNER, E. 1967. Ultrastructure of spontaneous hyperplastic nodules in mouse liver. *Cancer Res.* **27**:2137.
11. FARBER, E. 1956. Similarities in the sequence of early histologic changes induced in the liver of the rat by ethionine, 2-acetyl aminofluorene and 3′-methyl-4-dimethyl-aminoazobenzene. *Cancer Res.* **16**:142.
12. GRISHAM, J. W., and E. A. PORTA. 1964. Origin and fate of proliferated hepatic ductal cells in the rat: electron microscopic and autoradiographic studies. *Exp. Mol. Pathol.* **3**:242.
13. HAY, E. D., and D. A. FISHMAN. 1960. Origin of the blastema in regenerating limbs of the newt *Triturus viridescens*. *Develop. Biol.* **3**:26.
14. HOWATSON, A. F., and A. W. HAM. 1955. Electron microscope study of sections of two rat liver tumors. *Cancer Res.* **15**:62.
15. HRUBAN, Z., H. SWIFT, and M. RECHCIGL, JR. 1965. Fine structure of transplantable hepatomas of the rat. *J. Nat. Cancer Inst.* **35**: 459.
16. INAOKA, Y. 1967. Significance of the so-called oval cell population during azo-dye hepatocarcinogenesis. *Gann.* **58**:355.
17. JONES, O. P. 1962. Paramitotic granulation and ribosome bodies in erythroblasts. *J. Ultrastruct. Res.* **7**:308.
18. KARASAKI, S. 1965. Electron microscopic examination for the sites of nuclear RNA synthesis during amphibian embryogenesis. *J. Cell Biol.* **26**:937.
19. KARASAKI, S. 1967. An electron microscope study on neoplastic transformation in rat liver parenchyma. *Proc. Amer. Ass. Cancer Res.* **8**:35.
20. LAFONTAINE, J-G., and C. ALLARD. 1964. A light and electron microscope study of the morphological changes induced in rat liver cells by the azo dye 2-Me-DAB. *J. Cell Biol.* **22**:143.
21. MA, M. H., and A. J. WEBBER. 1966. Fine structure of liver tumors induced in the rat by 3′-methyl-4-dimethyl-aminoazobenzene. *Cancer Res.* **26**:935.
22. MACDONALD, R. A. 1961. Experimental carcinoma of the liver. "Regeneration" of liver cells in premalignant stages. *Amer. J. Pathol.* **39**:209.
23. MERKOW, L. P., S. M. EPSTEIN, B. J. CAITO, and B. BARTUS. 1967. The cellular analysis of liver carcinogenesis: Ultrastructural alterations within hyperplastic liver nodules induced by 2-fluorenylacetamide. *Cancer Res.* **27**:1712.
24. MILLER, E. C., J. A. MILLER, B. E. KLINE, and H. P. RUSEH. 1948. Correlation of the level of hepatic riboflavin with the appearance of liver tumors in rats fed aminoazo dyes. *J. Exp. Med.* **88**:89.
25. MOLNAR, F., and R. DAOUST. 1965. Nucleocytoplasmic ratios in rat liver parenchyma during DAB carcinogenesis. *Cancer Res.* **25**:1213.
26. MOULÉ, Y. 1964. Endoplasmic reticulum and microsomes of rat liver. *In* Cellular Membranes in Development. N. Locke, editor. Academic Press Inc., New York. 97.
27. NOVIKOFF, A. B., and E. ESSNER. 1960. The Liver cell. *Amer. J. Med.* **29**:102.
28. OBERLING, C., and W. BERNHARD. 1961. The morphology of cancer cells. *In* The Cell. J. Brachet and A. E. Mirsky, editors. Academic Press Inc., New York. **5**:405.

29. ONOÉ, T., and Y. FUSE. 1966. Electron microscopic study of azo-dye carcinogenesis. *Tumor Res.* **1**:143.
30. OPIE, E. L. 1946. Mobilization of basophilic substance (ribonucleic acid) in the cytoplasm of liver cells with the production of tumors by butter yellow. *J. Exp. Med.* **84**:91.
31. ORR, J. W. 1940. The histology of the rat's liver during the course of carcinogenesis by butter yellow. *J. Pathol. Bacteriol.* **50**:392.
32. PALADE, G. E., and P. SIEKEVITZ. 1956. Liver microsomes; an integrated morphological and biochemical study. *J. Biophys. Biochem. Cytol.* **2**:171.
33. PORTER, K. R., and C. BRUNI. 1959. An electron microscopic study of the early effects of 3'-methyl-4-dimethylaminoazobenzene on rat liver cells. *Cancer Res.* **19**:987.
34. ROUILLER, C. 1964. Experimental toxic injury of the liver. *In* The Liver. C. Rouiller, editor. Academic Press Inc., New York. **2**:335.
35. ROUILLER, C., and A. M. JÉZÉQUEL. 1963. Electron microscopy of the liver. *In* The Liver. C. Rouiller, editor. Academic Press Inc., New York. **1**:195.
36. SIMARD, A., and R. DAOUST. 1966. DNA synthesis and neoplastic transformation in rat liver parenchyma. *Cancer Res.* **26**:1665.
37. STEINER, J. W., Z. M. PERZ, and L. B. TAICHMAN. 1966. Cell population dynamics in the liver. A review of quantitative morphological techniques applied to the study of physiological and pathological growth. *Exp. Mol. Pathol.* **5**:146.
38. STENGER, R. J., and D. B. CONFER. 1966. Hepatocellular ultrastructure during liver regeneration after subtotal hepatectomy. *Exp. Mol. Pathol.* **5**:455.
39. SVOBODA, D. J. 1964. Fine structure of hepatomas induced in rats with p-dimethylaminoazobenzene. *J. Nat. Cancer Inst.* **33**:315.